

# DELNET: CONTINUOUS ALL-IN-ONE WEATHER REMOVAL VIA DYNAMIC EXPERT LIBRARY

Shihong Liu<sup>1</sup>, Kun Zuo<sup>2</sup>, Hanguang Xiao<sup>1\*</sup>

<sup>1</sup>School of Artificial Intelligence, Chongqing University of Technology, Chongqing 401135, China

<sup>2</sup>Sun Yat-sen University, Shenzhen Campus, Shenzhen, Guangdong 518107, China

52232313112@stu.cqut.edu.cn, zuok@mail2.sysu.edu.cn

simenxiao1211@163.com

\* Corresponding author

## ABSTRACT

All-in-one weather image restoration methods are valuable in practice but depend on pre-collected data and require retraining for unseen degradations, leading to high cost. We propose DELNet, a continual learning framework for weather image restoration. DELNet integrates a judging valve that measures task similarity to distinguish new from known tasks, and a dynamic expert library that stores experts trained on different degradations. For new tasks, the valve selects top-k experts for knowledge transfer while adding new experts to capture task-specific features; for known tasks, the corresponding experts are directly reused. This design enables continuous optimization without retraining existing models. Experiments on OTS, Rain100H, and Snow100K demonstrate that DELNet surpasses state-of-the-art continual learning methods, achieving PSNR gains of 16%, 11%, and 12%, respectively. These results highlight the effectiveness, robustness, and efficiency of DELNet, which reduces retraining cost and enables practical deployment in real-world scenarios.

**Index Terms**— All-in-one image restoration, Mixture-of-Experts, Continue learning, Adverse weather removal

## 1. INTRODUCTION

Adverse weather restoration has evolved from single-task models (rain, fog, snow, low-light, etc.) to all-in-one networks [1–4]. However, existing methods either rely on multiple encoders-decoders with high switching cost or unified structures that overlook degradation differences, both lacking continual learning. This limits deployment in dynamic environments such as autonomous driving [5].

Continual learning [6] enables adaptation to new tasks but suffers from catastrophic forgetting. Memory-based solutions [7] partially alleviate this issue but introduce high overhead and limited feature diversity.

To overcome these challenges, we propose the Dynamic Expert Library Network (DELNet) (Fig. 1 d), which integrates a judging valve to identify task similarity, a dynamic

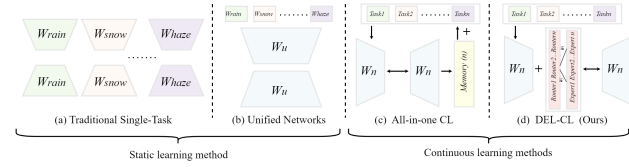


**Fig. 1.** Comparison chart of methods for eliminating adverse weather conditions. Including single removal method, unified method, all-in-one continuous learning method and our method.

expert library to preserve old knowledge while adding new experts, and a feature enhancement backbone to improve restoration quality. This design achieves continual adaptation without forgetting, enabling robust multi-weather image restoration.

## 2. METHODS

### 2.1. Overall architecture

The overall architecture of DELNet (Fig. 2) consists of a Deep Feature Enhancement (DFE) network, a judging valve, and a dynamic expert library. The DFE employs parallel self-attention and polarization attention with soft maximization and weight mapping to strengthen channel-spatial features for high-quality restoration. The judging valve generates task feature vectors, compares them with historical tasks, and classifies each as new or old. For new tasks, top-k experts are selected and updated with new adapters; for old tasks, corresponding experts are reused. Finally, outputs of active experts are fused, performance scores are updated, and trained experts are frozen to prevent forgetting, enabling continual learning across diverse weather degradations.

### 2.2. Judging Valve

Typical MoE adapters [8, 9] require manually defined task representations to activate routers. To address this limita-

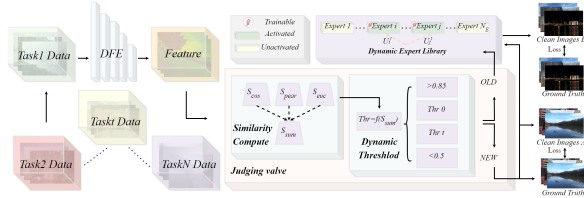


**Fig. 2.** Overview of DELNet. The framework integrates a Deep Feature Enhancement (DFE) network, a judging valve, and a dynamic expert library for continual multi-weather image restoration.

tion, we propose the Judging Valve (JV), which automatically identifies and classifies input tasks without manual intervention.

**Feature Vectors and Similarity.** For each task  $Task_t$ , features from the backbone are summarized into a task vector  $T^t$  using five statistics: mean, standard deviation, maximum, minimum, and  $L_2$  norm. Task similarity is then computed by a combined metric  $S_{sum}$ , integrating cosine similarity  $S_{cos}$ , Euclidean similarity  $S_{euc}$ , and Pearson similarity  $S_{pear}$ . This enables DELNet to decide whether the current task is new or old. The process is formulated as:

$$S_{cos}(T^1, T^2) = \frac{T^1 \cdot T^2}{\|T^1\|_2 \|T^2\|_2}, \quad (1)$$

$$\|T^t\|_2 = \left( \sum_{k=1}^d (t_k^t)^2 \right)^{1/2}, \quad (2)$$

where  $T^1 \cdot T^2 = \sum_{k=1}^d t_k^1 t_k^2$  is the dot product of two vectors,  $t_k^t$  is the  $k$ -th element of  $T^t$ , and  $d$  is the vector dimension.

The Euclidean similarity is obtained from the distance

$$d_{euc} = \|T^1 - T^2\|_2, \quad S_{euc} = \frac{1}{1 + d_{euc}}, \quad (3)$$

while the Pearson similarity  $S_{pear}$  measures the linear correlation between task vectors. Finally, the overall similarity is expressed as

$$S_{sum} = a \cdot S_{cos} + b \cdot S_{euc} + c \cdot S_{pear}, \quad (4)$$

with weights  $a = 0.5$ ,  $b = 0.3$ , and  $c = 0.2$ .

**Dynamic threshold management.** To enhance adaptability, DELNet employs a dynamic threshold mechanism based on historical task similarities. The first task is initialized as new with similarity 1.0 and threshold 0.75. For later tasks, similarity  $> 0.85$  indicates old,  $< 0.5$  indicates new, while intermediate cases trigger threshold updates once samples exceed three. The update is defined as:

$$Thr_0 = MS_{sum} - 0.25 \times STS_{sum}, \quad (5)$$

where  $MS_{sum}$  and  $STS_{sum}$  are the median and standard deviation of similarities. The decision boundary is then adaptively updated:

$$Thr_{t+1} = Thr_t + e \times \text{clip}(Thr_0, -f, f), \quad (6)$$

with  $e = 0.05$  controlling update speed and  $f = 0.05$  bounding changes for stability. In practice, we further include skewness and kurtosis statistics to improve task separability, and bound the dynamic threshold within  $[0.65, 0.90]$  for stability.

### 2.3. Dynamic Expert Library

**Definition of Dynamic Expert Library.** The Dynamic Expert Library (DEL) is a scalable MoE-based architecture [10] designed to mitigate catastrophic forgetting. Each expert is implemented as a lightweight adapter composed of instance normalization, projection convolutions, activation, and residual connection. Every expert maintains an independent parameter set and evaluation metric, tailored for specific degradations such as rain, snow, or fog. Formally, the expert set is defined as:

$$\{\varepsilon_i\}_{i=1}^{N_E}, \quad (7)$$

where  $N_E$  is the number of experts (30 in our implementation, adjustable by task scale).

**Expert scheduling selection.** DEL employs a performance–usage joint score with Top- $K$  selection to activate only the most relevant experts, while freezing the others (Fig. 3). For a new task, each expert is assigned a score:

$$S_c = P_i \times U_i = P_i \times \frac{1}{C_i + \epsilon}, \quad (8)$$

where  $P_i$  is the performance score,  $C_i$  the usage frequency, and  $\epsilon = 10^{-6}$  ensures stability.  $P_i$  is updated by an exponential moving average:

$$P^{(t+1)}(i) = \beta_t \cdot P^t(i) + (1 - \beta_t) \cdot \frac{1}{L_i + \epsilon}. \quad (9)$$

with  $\beta_t = 0.9$  and  $L_i$  the task loss.

The weights of selected experts are computed by loss-based temperature scaling:

$$u_i = \frac{\exp(-L_i/\tau)}{\sum_{j=1}^K \exp(-L_j/\tau)}. \quad (10)$$

where  $\tau = 0.1$  and  $K$  is the number of active experts. The final output is the weighted fusion:

$$y = \sum_{i=1}^K u_i \cdot E_i(x), \quad (11)$$

with  $E_i(x)$  denoting the transformation of expert  $i$  on input  $x$ .

### 2.4. Loss function combination strategy

We design a multi-level objective to promote knowledge transfer and retention: (i) reconstruction and contrastive losses for pixel fidelity and semantic consistency; (ii) output-level distillation and feature-level projection to mitigate forgetting; and (iii) adapter regularization with a dynamic coefficient, complemented by a lightweight expert-diversity term.

#### Reconstruction & contrastive.

$$L_{sw}^{(0)} = \|I_{pred} - I_{gt}\|_1, \quad (12)$$

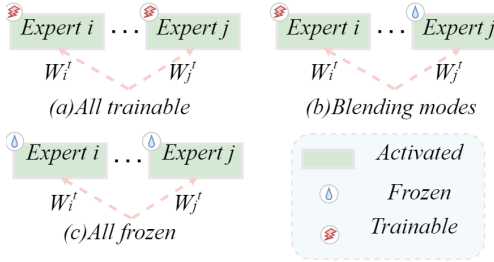


**Fig. 3.** Three different adapter and expert modes: (a) All trainable, (b) Blending modes, and (c) All frozen.

$$L_c = \text{ContrastLoss}(I_{pred}, I_{gt}, I_{input}), \quad (13)$$

$$L_{sw} = L_{sw}^{(0)} + \beta_1 L_c. \quad (14)$$

#### Distillation (output-level).

$$L_{kd}^{(0)} = \|I_{pred.old} - I_{pred.new}\|_1, \quad (15)$$

$$L_{kd} = L_{kd}^{(0)} + \beta_2 \text{ContrastLoss}(I_{pred.new}, I_{pred.old}, I_{old}). \quad (16)$$

#### Projection (feature-level).

$$h_{old} = \text{AutoEncoder.pjt}(f_{old}),$$

$$h_{new} = \text{AutoEncoder.pjt}(f_{new}), \quad (17)$$

$$L_p = \|h_{old} - h_{new}\|_1.$$

#### Regularization (adapters).

$$L_{reg} = \sum_{i=1}^N \|\omega_i\|_2, \quad \beta = 0.01 \cdot \min\left(\frac{\text{step}}{\text{steps}\cdot 5}, 0.1\right). \quad (18)$$

#### Diversity (experts).

$$L_{div} = -\gamma \cdot \text{Std}\{L_i\}_{i=1}^K, \quad \gamma = 0.01, \quad (19)$$

where  $L_i$  is the loss of the  $i$ -th active expert among  $K$  selected experts. This term encourages specialization and reduces redundancy with negligible overhead.

#### Total.

$$L_{total} = L_{sw} + \alpha L_{kd} + \lambda L_{reg} + L_{div}, \quad (20)$$

*Notation.*  $I_{pred}$ : model output;  $I_{gt}$ : ground truth;  $I_{input}$ : degraded input.  $I_{pred.old}/I_{pred.new}$ : outputs of old (teacher) / current model on the same old data  $I_{old}$ .  $f_{old}/f_{new}$ : encoder features;  $h_{old}/h_{new}$ : their projected features.  $\omega_i$ : weight of the  $i$ -th adapter's projection layer;  $N$ : number of adapters.  $\beta_1, \beta_2$ : contrastive weights;  $\beta$ : dynamic regularization weight. We set  $\alpha = 0.8$  and  $\lambda = 0.3$  empirically.

## 3. EXPERIMENT

### 3.1. Datasets and Settings

We evaluate on RESIDE (haze), Rain100H (rain), and Snow100K (snow) following the order haze→rain→snow. Training uses Adam ( $lr = 2 \times 10^{-4}$ , cosine decay) for  $5 \times 10^5$  iterations, batch size 2, crop size  $240 \times 240$ . Evaluation adopts PSNR and SSIM on official test sets. All reported results are from

Methods	Avg	OTS	Rain100H	Snow100K
EWC [11]	<b>27.79/0.81</b>	28.23/0.86	<b>25.99/0.76</b>	29.16/0.80
MAS [12]	25.74/0.73	<b>29.11/0.94</b>	20.68/0.51	27.45/0.73
LwF [13]	20.90/0.64	23.12/0.86	15.24/0.36	24.35/0.71
POD [14]	22.80/0.66	23.19/0.82	16.56/0.40	28.65/0.77
PIGWM [15]	23.31/0.71	28.33/0.94	15.16/0.48	26.45/0.73
AFC [16]	25.73/0.77	26.73/0.83	20.48/0.66	<b>29.98/0.82</b>
DELNet (Ours)	<b>31.28/0.94</b>	<b>31.22/0.98</b>	<b>29.03/0.89</b>	<b>33.58/0.94</b>
TransWeather [17]	27.82/0.88	27.12/0.91	28.53/0.88	27.83/0.85
WGWS [18]	29.61/0.91	29.54/0.94	<b>29.10/0.88</b>	30.19/0.90
Chen et al. [19]	27.66/0.87	27.34/0.90	28.69/0.87	26.97/0.82
AIRFormer [20]	26.04/0.85	25.67/0.95	24.46/0.74	28.01/0.85
WeatherDiff [21]	29.94/0.90	24.30/0.95	26.66/0.85	28.86/0.89
ADSM [22]	30.21/0.91	30.66/0.92	<b>29.74/0.89</b>	30.24/0.91
CLAIO [7]	<b>30.67/0.93</b>	<b>31.05/0.98</b>	28.66/0.88	<b>32.31/0.93</b>
DELNet (Ours)	<b>31.28/0.94</b>	<b>31.22/0.98</b>	29.03/0.89	<b>33.58/0.94</b>

**Table 1.** Haze, rain, and snow removal in the single-task sequence. Top: continual learning methods. Bottom: integrated methods. Results in PSNR/SSIM, best in red, second best in blue.

Methods	Avg	OTS	Rain100H	Snow100K
EWC [11]	24.61/0.71	27.69/0.78	20.69/0.63	25.47/0.73
MAS [12]	24.74/0.79	26.38/0.90	23.15/0.69	24.71/0.77
LwF [13]	21.41/0.70	21.85/0.86	16.99/0.42	25.40/0.81
POD [14]	23.60/0.78	23.66/0.83	18.35/0.70	<b>28.81/0.81</b>
PIGWM [15]	24.44/0.87	<b>28.93/0.95</b>	17.44/0.81	26.95/0.85
AFC [16]	<b>26.96/0.83</b>	27.94/0.82	<b>24.84/0.87</b>	28.10/0.81
DELNet	<b>29.69/0.91</b>	<b>30.06/0.94</b>	<b>28.74/0.88</b>	<b>30.29/0.91</b>
TransWeather [17]	27.82/0.88	27.12/0.91	28.53/0.88	27.83/0.85
WGWS [18]	29.61/0.91	29.54/0.94	<b>29.10/0.88</b>	30.19/0.90
Chen et al. [19]	27.66/0.87	27.34/0.90	28.69/0.87	26.97/0.82
AIRFormer [20]	26.04/0.85	25.67/0.95	24.46/0.74	28.01/0.85
WeatherDiff [21]	<b>29.94/0.90</b>	24.30/0.95	26.66/0.85	28.86/0.89
ADSM [22]	<b>30.21/0.91</b>	<b>30.66/0.92</b>	<b>29.74/0.89</b>	<b>30.24/0.91</b>
CLAIO [7]	29.54/0.90	<b>30.47/0.93</b>	28.11/0.87	30.05/0.90
DELNet	29.69/0.91	30.06/0.94	28.74/0.88	<b>30.29/0.91</b>

**Table 2.** Results of haze, rain, and snow removal using multi-task sequence (others same as Table 1)

the full training setup; a lightweight debug configuration is provided in code but not used for tables.

### 3.2. Method comparison

We evaluate DELNet under two settings: single-task sequence (tasks trained/tested sequentially) and multi-task sequence (tasks jointly trained/tested), following CLAIO [7]. Comparisons include continual learning baselines [11–16] and static all-in-one models [17, 18, 21], using official codes and identical datasets. Results are reported in Table 1, Table 2, and Fig. 4.

DELNet achieves consistent gains: on single-task sequences it improves PSNR by 2.11–3.54dB over continual baselines and up to 1.27dB over static methods, reaching 29.03dB on Rain100H (vs. 29.74dB best). It produces clearer targets with natural lighting while requiring only 5.6M parameters, far fewer than TransWeather (38.1M), WeatherDiff (83.0M), and WGWS (6M) (Table 3). On mixed rain-fog data, it further surpasses the second-best by +0.14dB / +0.0112 SSIM and the strongest static baseline by +4.95dB. These results confirm DELNet’s robustness, efficiency, and adaptability under continual learning.

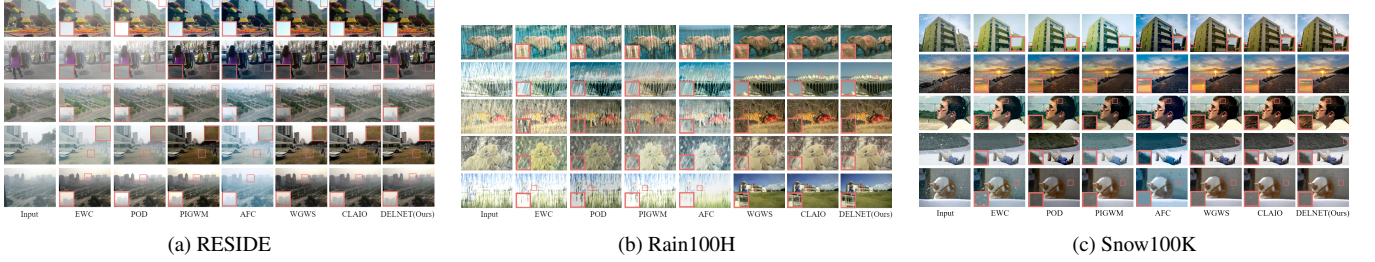


**Fig. 4.** Visualization of image restoration results on RESIDE, Rain100H, and Snow100K datasets.

Methods	Outdoor-Rain (PSNR/SSIM)	Params
All-in-One [23]	24.71/0.8980	44.0M
TransWeather [17]	28.83/0.9000	38.1M
AirNet [24]	25.69/0.8993	—
Chen et al. [19]	23.94/0.8500	28.7M
WGWS [18]	25.32/0.9070	6.0M
LDR [25]	26.92/0.9120	—
AIRFormer [20]	24.52/0.7837	—
WeatherDiff [21]	25.78/0.8990	83.0M
ADSM [22]	<b>29.52/0.9015</b>	—
CLAIO [7]	26.78/0.9199	8.2M
DELNet (Ours)	<b>29.66/0.9311</b>	<b>5.6M</b>

**Table 3.** Outdoor-Rain dataset (deraining + dehazing). Results reported as PSNR/SSIM (baselines same as in Section 3.2).

**Table 4.** The melting results of components in the overall network.

Combination	FFA	DFE	JV	DEL	PSNR	SSIM
Baseline	—	—	—	—	13.83	0.4267
C1	✓	—	—	—	16.71	0.7914
C2	—	✓	—	—	17.32	0.7974
C3	—	✓	✓	—	24.76	0.8125
C4	—	✓	✓	✓	<b>31.22</b>	<b>0.9784</b>

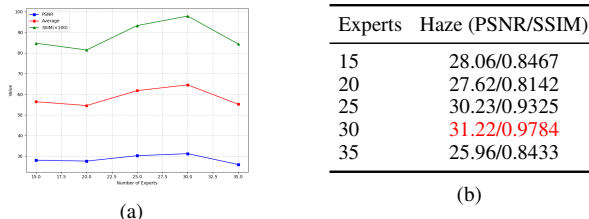


**Fig. 5.** Ablation on expert number: (a) Impact of the number of experts (b) Ablation on expert number (Haze).

### 3.3. Ablation study

We conduct ablation studies on the OTS dehazing dataset [26] to validate the effectiveness of each module and loss design. As shown in Table 4, integrating the judging valve, DFE, and dynamic expert library yields the best performance. Figure 6 further visualizes feature extraction, where snow patterns are clearly captured and removed. Figure 5 analyze the number of experts: increasing experts enhances knowledge capacity and PSNR/SSIM, but also raises training cost; around 30 experts provides the best trade-off. Table 5 compares differ-

**Table 5.** Experimental results of ablation using different loss functions.

Loss	Lsw	Lkd	Lp	Lreg	Lct	PSNR	SSIM
C5	✓	—	—	—	—	25.97	0.8486
C6	✓	✓	—	—	—	28.99	0.9072
C7	✓	✓	✓	—	—	29.97	0.9354
C8	✓	✓	✓	✓	—	29.99	0.9691
C9	✓	✓	✓	✓	✓	<b>31.22</b>	<b>0.9784</b>

Task Seq.	Avg	OTS	Rain100H	Snow100K
rain-snow-haze	29.58/0.93	28.19/ <b>0.98</b>	<b>29.65</b> /0.89	30.90/0.91
rain-haze-snow	29.37/0.93	28.11/0.97	29.07/ <b>0.89</b>	30.94/0.92
haze-snow-rain	29.77/0.92	29.58/0.95	28.35/0.87	31.40/ <b>0.93</b>
haze-rain-snow	29.69/0.91	<b>30.06</b> /0.94	28.74/0.88	30.29/0.91
snow-rain-haze	<b>30.21</b> /0.93	29.45/0.97	<b>29.11</b> / <b>0.89</b>	<b>32.09</b> /0.93
snow-haze-rain	<b>30.26</b> /0.93	<b>29.70</b> / <b>0.97</b>	29.03/0.89	<b>32.06</b> /0.93

**Table 6.** Continual learning under different task orders (PSNR/SSIM).

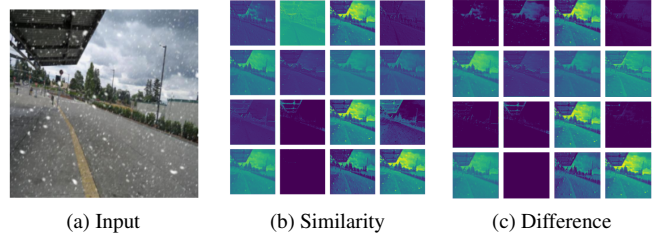


**Fig. 6.** Visualization of feature maps for extracting intermediate features in rainy weather.

ent loss combinations, confirming that multi-level supervision achieves optimal results. Finally, Table 6 explores different task sequences, showing that task order significantly affects continual learning, with earlier tasks achieving better performance. This highlights task-order sensitivity as an open challenge for future work.

## 4. CONCLUSION

We introduced DELNet, a continual learning framework for all-weather restoration. With a judging valve, dynamic expert library, and multi-level objective, DELNet mitigates forgetting and adapts to new degradations without retraining. Experiments show consistent gains over baselines. Future work

will focus on efficient teacher updating and robustness under extreme conditions.

## Acknowledgement

This work was supported by the National Natural Science Foundation of China (Grant No. 62471075), the Chongqing's "Tender-Based System" Project Initiative in the Field of Industry and Information Technology (Grant No. YJX202500-1001002), the Natural Science Foundation of Chongqing (Grant No. CSTB2024NSCQ-LZX0080, CSTB2023TI AD-STX0020, CSTB2025NSCQ-LZX0115, CSTB2023NS CQ-LZX0068, CSTB2022NSCQ-MSX0837). This study does not involve any ethical issue.

## 5. REFERENCES

- [1] Wei Sun, Qianzhou Wang, Yaqi Wang, Zhiqiang Hou, Qingsen Yan, and Yanning Zhang, "Adaprompt-ir: Adaptive learning to perceive degradation semantic and prompting for all-in-one image restoration," *Pattern Recognition*, vol. 169, pp. 111875, 2026.
- [2] Weichao Yi, Liqian Dong, Ming Liu, Lingqin Kong, Yue Yang, Xuhong Chu, and Yuejin Zhao, "Multi-stage dehazing network: Where haze perception unit meets global and local progressive contrastive regularization," *Expert Systems with Applications*, vol. 270, pp. 126549, 2023.
- [3] Yuanbo Wen, Tao Gao, Jing Zhang, Ziqi Li, and Ting Chen, "Multi-axis prompt and multi-dimension fusion network for all-in-one weather-degraded image restoration," in *Proceedings of the AAAI Conference on Artificial Intelligence*, 2025, vol. 39, pp. 8323–8331.
- [4] Ziqiang Shi and Ruijie Liu, "Noisy image restoration based on conditional acceleration score approximation," in *ICASSP 2024 - 2024 IEEE International Conference on Acoustics, Speech and Signal Processing (ICASSP)*, 2024, pp. 4000–4004.
- [5] Xuan Xiong, Yicheng Liu, Tianyuan Yuan, Yue Wang, Yilun Wang, and Hang Zhao, "Neural map prior for autonomous driving," in *Proceedings of the IEEE/CVF Conference on Computer Vision and Pattern Recognition (CVPR)*, June 2023, pp. 17535–17544.
- [6] Donghyun Kim, Yungyeo Kim, and Joon-Hyuk Chang, "Class: Continual learning approach for speech super-resolution," in *ICASSP 2024 - 2024 IEEE International Conference on Acoustics, Speech and Signal Processing (ICASSP)*, 2024, pp. 1401–1405.
- [7] De Cheng, Yanling Ji, Dong Gong, Yan Li, Nannan Wang, Junwei Han, and Dingwen Zhang, "Continual all-in-one adverse weather removal with knowledge replay on a unified network structure," *IEEE Transactions on Multimedia*, vol. 26, pp. 8184–8196, 2024.
- [8] Zitian Chen, Yikang Shen, Mingyu Ding, Zhenfang Chen, Hengshuang Zhao, Erik G. Learned-Miller, and Chuang Gan, "Mod-squad: Designing mixtures of experts as modular multi-task learners," in *Proceedings of the IEEE/CVF Conference on Computer Vision and Pattern Recognition (CVPR)*, June 2023, pp. 11828–11837.
- [9] Peng Gao, Shijie Geng, Renrui Zhang, Teli Ma, Rongyao Fang, Yongfeng Zhang, Hongsheng Li, and Yu Qiao, "Clip-adapter: Better vision-language models with feature adapters," *International Journal of Computer Vision*, vol. 132, no. 2, pp. 581–595, February 2024.
- [10] Yanqi Zhou, Tao Lei, Hanxiao Liu, Nan Du, Yanping Huang, Vincent Zhao, Andrew M Dai, zhifeng Chen, Quoc V Le, and James Laudon, "Mixture-of-experts with expert choice routing," vol. 35, pp. 7103–7114, 2022.
- [11] James Kirkpatrick, Razvan Pascanu, Neil Rabinowitz, Joel Veness, Guillaume Desjardins, Andrei A. Rusu, Kieran Milan, John Quan, Tiago Ramalho, Agnieszka Grabska-Barwinska, Demis Hassabis, Claudia Clopath, Dharshan Kumaran, and Raia Hadsell, "Overcoming catastrophic forgetting in neural networks," *Proceedings of the National Academy of Sciences*, vol. 114, no. 13, pp. 3521–3526, 2017.
- [12] Rahaf Aljundi, Francesca Babiloni, Mohamed Elhoseiny, Marcus Rohrbach, and Tinne Tuytelaars, "Memory aware synapses: Learning what (not) to forget," in *Proceedings of the European Conference on Computer Vision (ECCV)*, September 2018.
- [13] Zhizhong Li and Derek Hoiem, "Learning without forgetting," *IEEE transactions on pattern analysis and machine intelligence*, vol. 40, no. 12, pp. 2935–2947, 2017.
- [14] Arthur Douillard, Matthieu Cord, Charles Ollion, Thomas Robert, and Eduardo Valle, "Podnet: Pooled outputs distillation for small-tasks incremental learning," in *Computer Vision – ECCV 2020*, Andrea Vedaldi, Horst Bischof, Thomas Brox, and Jan-Michael Frahm, Eds., Cham, 2020, pp. 86–102, Springer International Publishing.
- [15] Man Zhou, Jie Xiao, Yifan Chang, Xueyang Fu, Aiping Liu, Jinshan Pan, and Zheng-Jun Zha, "Image de-raining via continual learning," in *Proceedings of the IEEE/CVF Conference on Computer Vision and Pattern Recognition (CVPR)*, June 2021, pp. 4907–4916.
- [16] Minsoo Kang, Jaeyoo Park, and Bohyung Han, "Class-incremental learning by knowledge distillation with adaptive feature consolidation," in *Proceedings of the IEEE/CVF Conference on Computer Vision and Pattern Recognition (CVPR)*, June 2022, pp. 16071–16080.
- [17] Jeya Maria Jose Valanarasu, Rajeev Yasarla, and Vishal M. Patel, "Transweather: Transformer-based restoration of images degraded by adverse weather conditions," in *Proceedings of the IEEE/CVF Conference on Computer Vision and Pattern Recognition (CVPR)*, June 2022, pp. 2353–2363.
- [18] Yurui Zhu, Tianyu Wang, Xueyang Fu, Xuanyu Yang, Xin Guo, Jifeng Dai, Yu Qiao, and Xiaowei Hu, "Learning weather-general and weather-specific features for image restoration under multiple adverse weather conditions," in *Proceedings of the IEEE/CVF Conference on Computer Vision and Pattern Recognition (CVPR)*, June 2023, pp. 21747–21758.
- [19] Wei-Ting Chen, Zhi-Kai Huang, Cheng-Che Tsai, Hao-Hsiang Yang, Jian-Jiun Ding, and Sy-Yen Kuo, "Learning multiple adverse weather removal via two-stage knowledge learning and multi-contrastive regularization: Toward a unified model," in *Proceedings of the IEEE/CVF Conference on Computer Vision and Pattern Recognition (CVPR)*, June 2022, pp. 17653–17662.
- [20] Tao Gao, Yuanbo Wen, Kaihao Zhang, Jing Zhang, Ting Chen, Lidong Liu, and Wenhan Luo, "Frequency-oriented efficient transformer for all-in-one weather-degraded image restoration," *IEEE Transactions on Circuits and Systems for Video Technology*, vol. 34, no. 3, pp. 1886–1899, 2024.
- [21] Ozan Özdenizci and Robert Legenstein, "Restoring vision in adverse weather conditions with patch-based denoising diffusion models," *IEEE Transactions on Pattern Analysis and Machine Intelligence*, vol. 45, no. 8, pp. 10346–10357, 2023.
- [22] Yuanbo Wen, Tao Gao, Ziqi Li, Jing Zhang, Kaihao Zhang, and Ting Chen, "All-in-one weather-degraded image restoration via adaptive degradation-aware self-prompting model," *IEEE Transactions on Multimedia*, vol. 27, pp. 3343–3355, 2025.
- [23] Ruoteng Li, Robby T. Tan, and Loong-Fah Cheong, "All in one bad weather removal using architectural search," in *Proceedings of the IEEE/CVF Conference on Computer Vision and Pattern Recognition (CVPR)*, June 2020.
- [24] Boyun Li, Xiao Liu, Peng Hu, Zhongqin Wu, Jiancheng Lv, and Xi Peng, "All-in-one image restoration for unknown corruption," in *Proceedings of the IEEE/CVF Conference on Computer Vision and Pattern Recognition (CVPR)*, June 2022, pp. 17452–17462.

[25] Hao Yang, Liyuan Pan, Yan Yang, and Wei Liang, “Language-driven all-in-one adverse weather removal,” in *Proceedings of the IEEE/CVF Conference on Computer Vision and Pattern Recognition (CVPR)*, June 2024, pp. 24902–24912.

[26] Boyi Li, Wenqi Ren, Dengpan Fu, Dacheng Tao, Dan Feng, Wenjun Zeng, and Zhangyang Wang, “Benchmarking single-image dehazing and beyond,” *IEEE Transactions on Image Processing*, vol. 28, no. 1, pp. 492–505, 2018.